PARAMETRIC MODELLING OF THE GEOLOGICAL CROSS SECTION FOR SHIELD TUNNEL DESIGN AND CONSTRUCTION

L. Li [1 2], K. Chen [1]*, J. Yu[3], J. Wang[4], H. Luo [1]

[1] School of Civil and Hydraulic Engineering, Huazhong University of Science and Technology, China – (linhao_li, chenkecm, luohbcem)@hust.edu.cn
[2] Institute of Artificial Intelligence, Huazhong University of Science and Technology, China – linhao_li@hust.edu.cn
[3] Wuhan Urban Construction Investment Development Group Co., Ltd, China – yujing_ren_2000@163.com
[4] China Railway 14th Bureau Group Co., Ltd, China – 110375369@qq.com

Commission IV, WG IV/9

KEY WORDS: Underground construction; Shield tunnel; Parametric modelling; Geological modelling; Cross section

ABSTRACT:

Geological information is indispensable for the design and construction of underground structures, especially for large-diameter shield tunnels. The geological cross-section is expected to be accurately and efficiently modelled to provide sufficient geological information for decision-making. However, the existing methods are usually time-consuming, and the calculation results cannot be intuitively understood by engineers. To meet this demand, this study attempts to develop a parametric modelling approach for the geological cross-section of tunnelling construction. The proposed approach consisted of four steps. In the first step, the borehole records from the geological investigation are converted into the DataFrame format. Then, each point is assigned a soil type label and soil property parameter to form a data framework. In the third step, the cross-section is generated in mesh type and divided into two parts. Finally, the mesh models are rendered to visualize the stratum sequence and soil property distribution. The proposed approach is applied to Lianghu tunnelling construction in Wuhan, China, for verification. The results show that the 11 geological cross-sections with ground water surfaces can be automatically modelled within 25 seconds, including stratum sequence identification and ground pressure calculation. The calculation results could be successively used in the tunnel structural analysis. Therefore, the proposed approach potentially promotes a data-driven technology for underground engineering construction.

1. INTRODUCTION

In recent years, the demand for large-diameter and long-distance shield tunnelling technology has increased due to the rapid development of underground construction. However, the delivery of shield tunnelling construction often faces complicated geology and uneven strata, which brings challenges to structural design and excavation construction. In such a situation, geological modelling should be conducted to facilitate stratum identification (Zhang, 2018) and soil property prediction (Gong, 2018). In the design stage, information on the stratum and underground water level can be used to determine the structure load. The water and soil pressure acting on the shield segments need to be calculated in accordance with the cover soil depth and underground water level. In the construction stage, the operation parameters of the tunnel boring machine (TBM) must refer to certain geotechnical parameters, such as the friction angle and cohesion (Xu, 2019), the indexes of which reflect the contact behavior between the stratum and shield segments.

The literature has focused on geological modelling technology for shield tunnel design and construction. Culí (2016) utilized hydrogeological models to analyse the TBM advance and to explore geological characterization in a real-time manner. Li (2020) adopted digital integration theory to combine the geological model with numerical simulation to consider the matter of uneven soil distribution. Muzik (2015) investigated the numerical modelling availability of various phenomena in anisotropic conditions from different interpolation methods. Yu (2020) proposed an unsupervised architecture to extract geological-related features. Except for complex stratum recognition, underground water conditions are also a serious factor to be considered during tunnel design and construction. For underwater shield tunnelling in karst ground, the presence of underground water flow sometimes makes backfill grouting difficult (Zhang, 2018). Therefore, geological modelling can reflect the uncertainty of actual tunnelling and illustrate hydrogeological conditions in correlating the structural performance of shield segments, both helping to enhance construction safety management.

However, existing geological modelling methods still have some limitations. First, the modelling procedures are of low efficiency because their adopted algorithms are usually time-consuming (Liu, 2019); hence, the spatial variability of soil properties cannot be represented in a time-dependent manner. Second, the integration level of geological data is not enough, and in many cases, the strata are identified by qualitative methods and used for visualization only. Although some methods apply quantitative identification, they are subject to the sparseness of sampled data from borehole records (Sava, 2011). Thus, the subsequent excavation works cannot be directly improved through data analysis. Third, the transverse cross-section region, such as the vertical plane of tunnelling or cutter head surface of the shield machine, has not received enough attention. Most geological modelling methods focus on the objects of longitudinal geology profiles. In fact, the transverse

* Corresponding author

geological cross-section has equal values to the longitudinal one during the structure design and excavation (Ocak, 2014).

This paper proposes a parametric modelling approach for the geological cross-section of tunnelling construction. During shield tunnel design and construction, the transverse geology profile can be accurately and efficiently modelled, and the modelling results provide sufficient geological information for decision-making.

The next section introduces the framework and main algorithms of the proposed approach. Subsequently, the implementation of this approach is illustrated through a real-life case of the Wuhan Lianghu tunnelling project. Finally, in accordance with the practical applications, the results are concluded and discussed.

2. METHODS

2.1 Framework

Figure 1 presents the workflow of the proposed modelling approach, which contains four main steps.

I) Creating a geologic borehole DataFrame. As the geological information originates from the borehole data in the geological investigation report, the DataFrame format is proposed to uniformly collect the information of borehole name, borehole locations, stratum sequences, and levels. At the same time, some indexes must be labelled and assigned parameters, which will be convenient for later calculation.

II) Parametric modelling for the target cross-section. The cross-section includes the transverse plane of tunnelling and the cut head surface of the TBM. These surface models are automatically generated along the tunnelling route and transformed to mesh type by gridding.

III) Maximum likelihood estimation of stratum sequences, which is based on the mesh model of the cross-section, and the soil distributions are analysed and predicted following the space coordinates relations to the borehole locations.

IV) Maximum likelihood estimation of soil properties. According to the known drilling samples, the soil properties of unknown areas in the cross-section can be predicted through geostatistical methods.

After these four steps, the stratum sequence and the soil property distribution of the cross-section can be exhibited clearly. This modelling approach also provides a visualization strategy based on the color rendering of the modelling results. The subsequent sections will introduce the technical details of the individual steps.

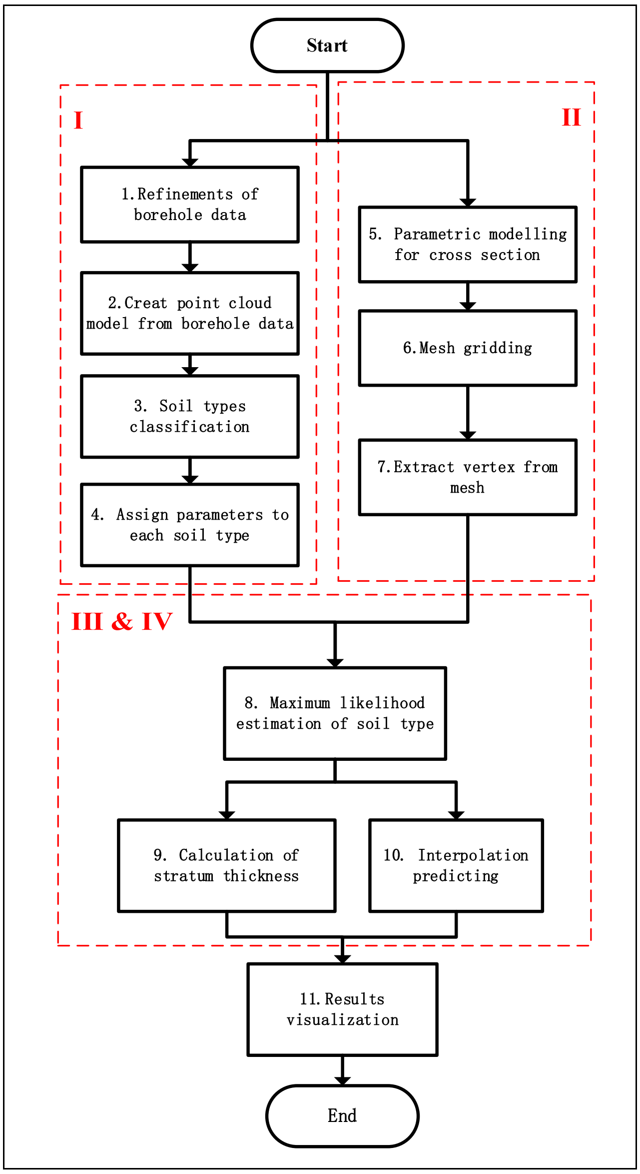

Figure 1. Workflow of the proposed approach

2.2 Creating geologic borehole DataFrame

Generally, geological drilling information is logged in geological investigation reports (see Table 1), where $D_{zk}[:,0]$ represents all of the row data of the 1st column in D_{zk}; $D_{zk}[:,1]$ represents all of the row data of the 2nd column in D_{zk}; and $D_{zk}[:,x]$ represents all of the row data of the x+1th column in D_{zk}.

Drilling No. ($D_{zk}[:,0]$)	*X* ($D_{zk}[:,1]$)	*Y* ($D_{zk}[:,2]$)	*Z* ($D_{zk}[:,3]$)	*SoilType* ($D_{zk}[:,4]$)
…	…	…	…	…

Table 1. Borehole data format

As one borehole has various soil distributions from the top layer to the bottom, the *z* parameters represent the top and bottom boundary for each stratum, and the borehole data can be collected in a DataFrame, D_{zk}. To subdivide the interval and improve the data density, **Algorithm 1** is proposed to give the function of automatic subdividing of borehole data to create Geological DataFrame, *D*, which has the same rows as D_{zk} but contains more points being regularly distributed. Thus, the subsequent calculations and predictions can achieve higher accuracy. The transformation from D_{zk} to D is illustrated in **Figure 2**. D can be represented through point cloud modelling with X, Y, Z parameters input and keeping the orders.

Input: The borehole data, D_{zk}; density of subdivision, *density*;
Output: The Geological DataFrame, D;
1. create a two-dimensional array in empty, S
2. calculate the number of boreholes, N_{zk}
3. **for** i **in** range(N_{zk}):
4. count up the amount of points in each borehole, N_d
5. divide the borehole depth with *density* into N points
6. **for** j **in** range(N_d):
7. create a depth interval between every two points in N_d that have the same *SoilType*, *(a, b)*
8. **for** f **in** range(N):
9. **if** f **in** *(a, b)*:
10. assign *SoiltType* to the fth point in N
11. put the fth point's *X, Y, Z* and *SoilType* in S
12. transform S into Dataframe, D
13. **return** D

Algorithm 1. Increasing data density of original geological information

D_{zk} =

	Drilling No.	*X*	*Y*	*Z*	*SoilType*
0	…	…	…	…	…
1	…	…	…	…	…
2	…	…	…	…	…
⋮	⋮	⋮	⋮	⋮	⋮
k	…	…	…	…	…

$\xrightarrow{\text{expanded}}$ D =

	Drilling No.	*X*	*Y*	*Z*	*SoilType*
0	…	…	…	…	…
1	…	…	…	…	…
2	…	…	…	…	…
⋮	⋮	⋮	⋮	⋮	⋮
k	…	…	…	…	…
⋮	⋮	⋮	⋮	⋮	⋮
n	…	…	…	…	…

Figure 2. Illustration of data processing

Normally, the geological investigation report provides the property parameters corresponding to the soil type, which are logged as Gauss mean values from testing on the examples. In this case, programing scripts can be used to assign these specific values to DataFrame D in an automatic manner. This procedure is illustrated in **Figure 3**.

D =

	Drilling No.	*X*	*Y*	*Z*	*SoilType*
0	…	…	…	…	…
1	…	…	…	…	…
2	…	…	…	…	…
⋮	⋮	⋮	⋮	⋮	⋮
k	…	…	…	…	…
⋮	⋮	⋮	⋮	⋮	⋮
n	…	…	…	…	…

$\xrightarrow{\text{refinded}}$ D_P =

	Drilling No.	*X*	*Y*	*Z*	*SoilType*	*Property*
0	…	…	…	…	…	…
1	…	…	…	…	…	…
2	…	…	…	…	…	…
⋮	⋮	⋮	⋮	⋮	⋮	⋮
k	…	…	…	…	…	…
⋮	⋮	⋮	⋮	⋮	⋮	⋮
n	…	…	…	…	…	…

Figure 3. The soil property parameters assignmentParametric modelling for the target cross section

The target cross-section includes two parts: one is the cutter head surface, and the other is the surrounding strata. The location of the section is dependent on the mileage of the tunnelling route. The section's size is adjusted to the diameter of tunnelling. During the excavation, these parameters are predesigned in the construction scheme and can be provided as input arguments for model generation. This study proposes **Algorithm 2** to show the procedures of parametric modelling.

As the created cross-section model is a boundary representation (Brep) object, it still needs to be processed with grid division for transformation into a mesh model. An illustration of the cross-section modelling and grid division is presented in **Figure 4**. Then, unduplicated nodes are retrieved from the mesh model, and their coordinates (as V) are regarded as the estimating objects for maximum likelihood estimations. They are also required to be stored in DataFrame format.

$$V = \begin{array}{c|ccc} & X & Y & Z \\ \hline 0 & \ldots & \ldots & \ldots \\ 1 & \ldots & \ldots & \ldots \\ \vdots & \vdots & \vdots & \vdots \\ \text{n} & \ldots & \ldots & \ldots \end{array}$$

Input: The tunnelling route object in 3D curve model, R; mileage parameter of the route, M; diameter of tunnelling cross-section, D_T; The Geological DataFrame, D;
Output: The cross-section model of tunnelling, CS;
1. Based on M to retrieve the corresponding point and tangent in curve R, as P and T
2. Find and retrieve the nearest borehole's attitude (the maximum z value) in D, as A
3. Based on P and X, Y vectors of T to create a plane, P_l
4. Based on P_l to create a rectangle area as R_a, with $2D_T$ width and defining its top side at A, foot at $-D_T$ below P
5. Divide R_a by subtracting a circle with diameter of D_T that is centered on P
6. The circle and the rest part in R_a are together defined as surface models, CS
7. **return** CS

Algorithm 2. Parametric modelling for the target cross-section

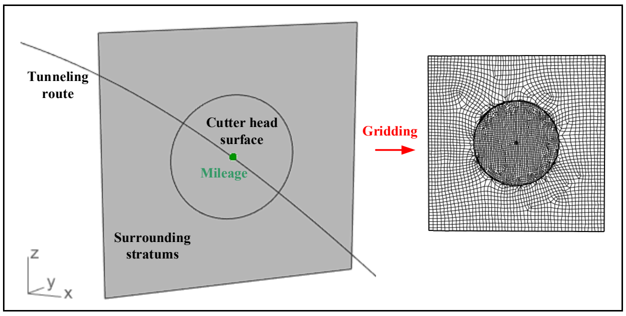

Figure 4. Illustration of the cross-section modelling and grid division

2.3 Stratum sequence estimation

To estimate the stratum sequences for each cross-section, the thickness and the boundary of each stratum must be obtained. With the retrieved unduplicated nodes, the nearest distances from them to the points of the borehole DataFrame should be calculated. Then, through the KNN (K-nearest neighbor) algorithm, the soil type for each node can be classified and labelled. In this way, the variable V is transformed into V' as follows.

$$V' = V+1 \begin{array}{c|c} & SoilType \\ \hline 0 & \cdots \\ 1 & \cdots \\ \vdots & \vdots \\ n & \cdots \end{array} = \begin{array}{c|cccc} & X & Y & Z & SoilType \\ \hline 0 & \cdots & \cdots & \cdots & \cdots \\ 1 & \cdots & \cdots & \cdots & \cdots \\ \vdots & \vdots & \vdots & \vdots & \vdots \\ n & \cdots & \cdots & \cdots & \cdots \end{array}$$

Then, a sampling statistics method is adopted to calculate the stratum thickness, and the buried depth is determined with the z value. **Algorithm 3** is proposed to give the functions of classifying and outputting the stratum sequences.

Input: The Geological DataFrame, *D*; unduplicated nodes in the cross section, *V*; neighbors' parameter of KNN algorithm, *k*
Output: classified nodes with soil type labelled, *V'*; the thickness of each stratum in the cross section, *SoilDepthList*

```
for i in range(rows of V):
    for j in range(rows of D):
        calculate the distance between V[i,:]and D[j,:]
    retrieve the nearest k neighbor points in D
    retrieve SoilType in the points and assign the frequent SoilType label to V[i,:] and generate V'[i,:]
calculate 10 highest z value in V'[i,:] and output the average value as A (approximately equal to An in Algorithm 2)
calculate 10 lowest z value for each kind of SoilType in V' and output the average value in a List
create an empty list as SoilDepthList
for i in range(length of List):
    SoilDepthList.append(List [i] - A)
    A = List[i]
return V' and SoilDepthList
```

Algorithm 3. Stratum sequence identification and thickness calculation

In addition, the prediction of the groundwater table is carried out in three steps.

I) retrieve the groundwater table parameter (h) of each drilling from the geological investigation report and combine the drilling locations X and Y to form a DataFrame W as follows.

$$W = \begin{array}{c|cccc} & drilling\ No. & X & Y & h \\ \hline 0 & \cdots & \cdots & \cdots & \cdots \\ 1 & \cdots & \cdots & \cdots & \cdots \\ 2 & \cdots & \cdots & \cdots & \cdots \\ \vdots & \vdots & \vdots & \vdots & \vdots \end{array}$$

II) using W as a data sample to train the ordinary kriging algorithm model with the help of programing language or program script execution. Then, the trained model is stored and transformed into a function for subsequent program invocation.

III) Define the target location or position with specific X,Y, and input X,Y into the trained ordinary kriging model to ultimately predict the target's groundwater table h.

To enable a more intuitive understanding of the modelling results, the cross-section model can be rendered with vertex color processing. Different colors can be applied to various types of *SoilType*. Additionally, the visualization of groundwater can be achieved by surface fitting in accordance with the predicted results.

2.4 Ground pressure determination

Combining the identified stratum sequences and the natural gravity parameters, the ground pressure acting on the shield linings can be determined in each cross-section. Normally, the pressure acts radially and can be divided into the vertical direction and horizontal direction. The horizontal ground pressure is dependent on the vertical earth pressure (Han et al., 2017). The vertical ground pressure could reflect the influence of the surrounding soil conditions on the shield lining design more directly. Thus, the ground pressure determination in this study mainly focuses on the vertical direction.

The vertical ground pressure acting on the crown of the lining can be determined as:

$$H = \sum H_i + \sum H_j \tag{1}$$

$$p_e = \sum \gamma_i H_i + \sum \gamma_j H_j \tag{2}$$

$$p_w = \gamma_w H_w \tag{3}$$

$$p = p_e + p_w \tag{4}$$

where H represents overburden, m; H_i is the thickness of i^{th} stratum over the tunnel, m; H_j is the thickness of j^{th} stratum over the tunnel, m; γ_i is natural gravity of soil in the i^{th} stratum,

https://doi.org/10.5194/isprs-annals-X-4-W2-2022-177-2022

kN/m^3; γ_j is natural gravity of soil in the j^{th} stratum, kN/m^3; P_e is earth pressure and P_w is water pressure, kPa; γ_w is natural gravity of groundwater, as 10 kN/m^3; H_w represents groundwater table, m; and P is the total pressure of P_e and P_w. These formulas are applicable to shallow sections. For deep sections, the pressure should be reduced following Terzaghi's theory.

2.5 Maximum likelihood estimation of soil property distribution

To estimate the soil property distribution in a space field, Markov or Gaussian geostatistical models are commonly used (Wang, 2018). However, considering the practical demands for calculation speed and easy manipulations, this study proposes to use the universal kriging model for estimations. The information of geological borehole data, including *X, Y, Z* and *property* parameters in D_p, is regarded as the input arguments for Universal Kriging model training. Unduplicated nodes from the cutter head surface are selected as the estimating objects (V). The trained universal kriging model is capable of estimating *property* parameters on the points of V. To visualize the estimated results, the parameter values are represented by a greyscale map in high to low order.

3. CASE STUDY

3.1 Project Overview

Wuhan Lianghu tunnelling project is one of the largest underwater highway shield tunnel projects in the urban area. According to the geological survey by CCCC Second Highway Engineering Bureau Co., Ltd., the excavation progress is mainly sited in the strata of weathered mudstone, tuffs, argillaceous sandstone, and silty clay, of which the uniaxial compressive strength widely changes from 2.15 MPa. The overburden is in the range of 10-42 m, and the tunnelling route has a minimum radius of 600 m and a 4.5% longitudinal gradient.

This case study focuses on a 100 m tunnelling section of QK2+820~QK2+920 and investigates the neighborhood geologic conditions by using the proposed modelling approach. In this way, 1) the surrounding strata in the minimum radius curve section can be identified with the most likelihood, which helps to consider the most unfavorable conditions for determining the segment lining design; 2) the earth pressure variation in front of the cutter head surface during excavating can be predicted, which is helpful for controlling the cutter chamber pressure and keeping the shield advance speed stable.

The selected parametric modelling tool is the Rhino & Grasshopper platform with the Python module plug-in. The configuration of the computer includes an Intel(R) Core(TM) i7–10700 CPU 2.90 GHz, 32 GB RAM, and an NVIDIA GeForce RTX 2060 SUPER GPU.

3.2 Strata identification and ground pressure

By creating the DataFrame and representing it with point clouds, the geologic borehole data were expressed in an intuitive way with the tunnel model incorporated (**Figure** 5). The drilling positions were distributed along the tunnelling route, and the separation distances were kept at 10-50 m. Using **Algorithm 1**, the subdivided DataFrame D with *SoilType* labelled is displayed below, and **Table** 2 gives explanations for the *SoilType*.

		Drilling No.	*X*	*Y*	*Z*	*SoilType*
	0	LH1X-ZK248	802400.812	382906.189	19.1	1-4
	1	LH1X-ZK248	802400.812	382906.189	18.6	1-4
	2	LH1X-ZK248	802400.812	382906.189	18.6	7-3
	3	LH1X-ZK248	802400.812	382906.189	18.1	7-3
$D=$	4	LH1X-ZK248	802400.812	382906.189	18.1	7-3
	5	LH1X-ZK248	802400.812	382906.189	17.6	7-3
	6	LH1X-ZK248	802400.812	382906.189	17.1	7-3
	7	LH1X-ZK248	802400.812	382906.189	17.1	10-1
	⋮	⋮	⋮	⋮	⋮	⋮
	7432	LH1X-ZK75	802676.783	382705.211	–37.8	20a-2

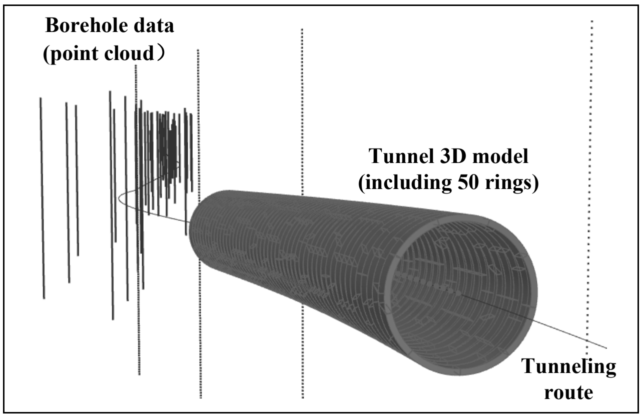

Figure 5. The geologic borehole data representation with tunnel model

Then, a cross-section was created and analysed at 10 m intervals in the section of QK2+820~QK2+920 and fitted to the groundwater surface (shown in **Figure** 6). The time consumption of this procedure is approximately 25 s, while each cross section needs 2.2 s for prediction and modelling. The modelling results illustrated that the excavation progress underpasses pebble and weathered mudstone layers. Such strata identification results conformed to the traditional analysis method from geological investigators, and the proposed modelling approach was demonstrated to make the results more explicit and understandable.

Based on the modelling results, the tunnelling progress would encounter composite strata after the mileage of QK2+840. The cutter head excavates the layers of pebbles, strongly weathered mudstone, and structural fracture zones. Normally, the pebble layer has a large water content and permeability coefficient, which may cause serious water leakage in shield segments. According to the geological investigation report, the compression modulus of these layers is stable and has a small difference, and these layers belong to the rock strata, where groundwater effusion should be carefully considered during excavation. In addition, the bottom of the linings in this section is located on the layers of moderately weathered mudstone and structural fracture zones. According to these analyses, validation of the tunnel longitudinal structure in this section should be further carried out to ensure the structural safety of the tunnel.

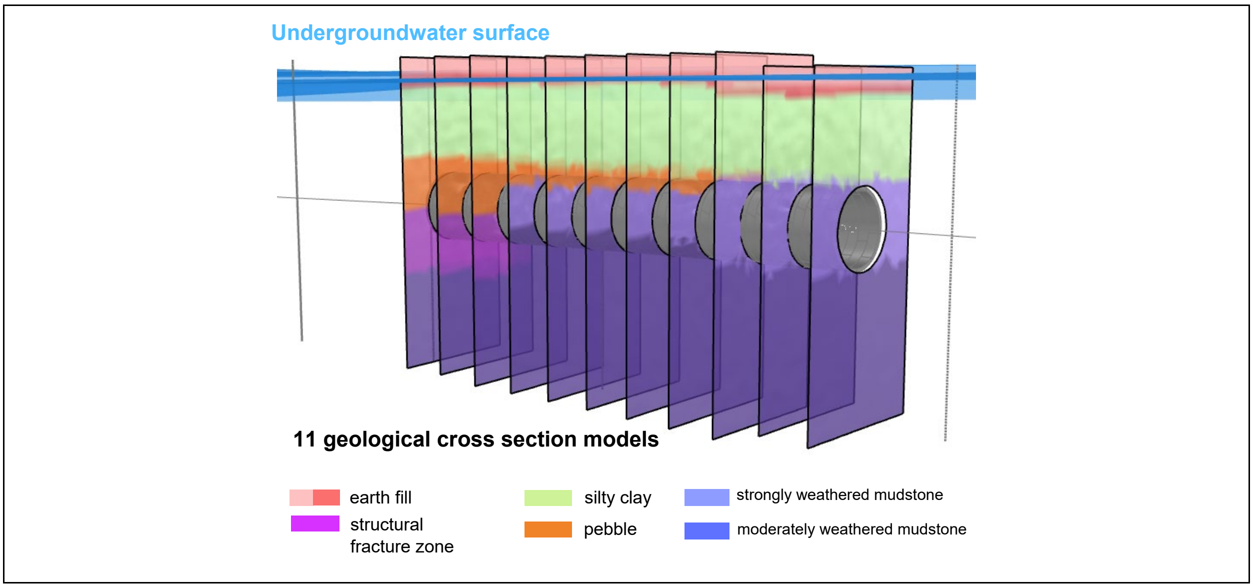

Figure 6. Geological cross-section modelled by the proposed parametric method

SoilType	Explanations	Natural gravity(kN/m^3)
1-1, 1-2	Earth fill	18.8
1-4	Mud	17.1
7-3	Clay	19.5
10-1	Silty clay	20
12c	Pebble	22
20a-1	Strongly weathered mudstone	25.7
20a-2	Moderately weathered mudstone	26.7
22	Structural fracture zone	25

Table 2. Soil type and property parameters in the original geological investigation report

Finally, each cross-section calculates its stratum thickness by using **Algorithm 3**, and the overburden with the groundwater table together was simultaneously determined by subtracting the tunnelling crown altitude in each cross-section (shown in **Figure** 7). This procedure is dependent on basic mathematics computing so that the time consumption is negligible. According to the results, the 10-20 m mileage would face a significant overburden growth from 19.79 m to 22.47 m. After 20 m, the pebble layer emerges and keeps the thickness increasing. The groundwater table also sees a continuous increase in the range of 17-20 m. Significantly, this tunnel section of 50 rings could have a changing ground pressure on the crown linings.

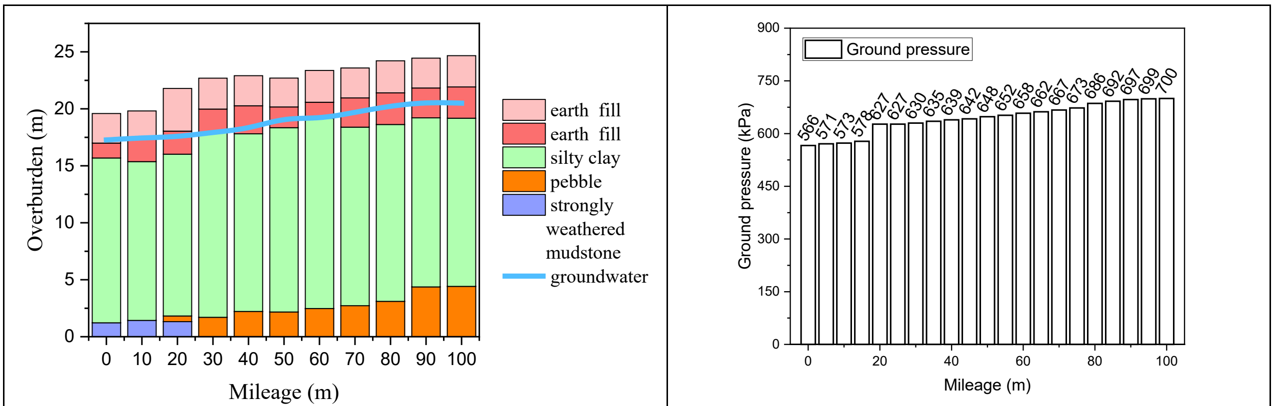

(a) overburden and groundwater table

(b) vertical ground pressure acts on the crown

Figure 7. Quantification of stratum sequences and ground pressure

By referring to the natural gravity parameters in **Table** 2, the ground pressure over the tunnel can be determined (see **Figure** 7b). In this case, study, the overburden is smaller than double the diameter (i.e., 29 m), and this tunnel section should be regarded as a shallow tunnel. Thus, Terzaghi's formula was not used. The interval between the two cross-sections was set at 5 m to clearly reflect the pressure variations. Along with tunnelling mileage, the pressure gradually increases from 566 kPa to 700 kPa, similar to the overburden growth. The ground pressure variation approximately conforms to the overburden growth rule. In addition, the ground pressure results are compared to geological surveys and design reports, and the discrepancy is below 10%. However, it is worth noting that other types of ground pressures, such as lateral arrangements or subgrade reactions, have not been considered in our method, and further improvements could be made on the basis of the proposed workflow to address these issues.

This parametric modelling method for 11 cross-section objects took approximately 25 seconds to visualize and calculate the ground pressure. Except for establishing DataFrame in the early stage, the entire modelling procedure was dependent on code manipulation and did not require any manual operations for parameter adjustment in each loop. Such a procedure makes the time consumption of our method shorter than existing methods (e.g., Graciano et al., 2018).

3.3 Soil property prediction

In this case, study, the natural gravity of soil was selected as the property parameter to be estimated since it can significantly influence the earth pressure acting on the cutter head surface horizontally during excavation. If the pressure on the head surface was too high, the excavation would bring an upheaval effect to the ground ahead; if the pressure was too low, the ground settlement would happen. Therefore, to help the TBM operators control the chamber pressure safely, it is necessary to provide them with real-time prediction of the natural gravity of soil ahead.

In the zone of QK2+820~QK2+920, the natural gravity variation in front of the 11 cutter head surfaces was analysed at 10 m intervals and was characterized by the peak and bottom values. At the same time, the cutter head surfaces were rendered with greyscale maps (seen in **Figure 8**). The Gauss mean values of related soils' natural gravity in the geologic investigation report can be found in **Table 2**. Compared with the mean values range of 22-25.7 kN/m^3 for the corresponding soils, the prediction results were in the range of 22.03-24.16 kN/m^3, showing slight divergences. From 0 to 100 m mileage, the discrepancy between the maximum and minimum limitations remained stable. At 50-70 m, the natural gravity was at a high level, which can be attributed to the composite strata of moderately weathered mudstone and pebble that emerged. With the help of the universal kriging algorithm, the trend of the natural gravity distribution on the surface can be easily explored. The values on the surface bottom were larger than the crown values, which can be explained by the historic layering effect. On this basis, the TBM operators should focus on adjusting the tunnelling parameters since the natural gravity increment may bring unstable earth pressure in front of the TBM and lead to uneven settlement on the ground. The natural gravity prediction on each cutter head surface contains two steps: model training and model calculation. Although the two steps progress in automatic algorithm operation, the former requires 2 hours, and the latter requires 6 hours for 11 cross sections. However, the time of modelling and rendering is less consuming. In this case, property prediction can be arranged at the preparatory stage of the project.

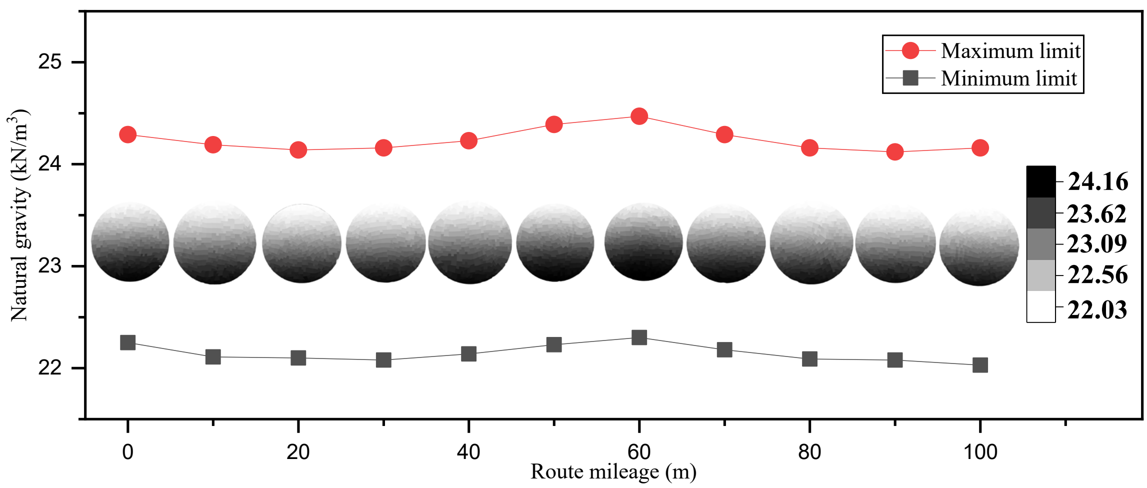

Figure 8. The cross-section modelling

4. CONCLUSION

This study presents a parametric modelling approach for stratum sequence identification and soil property prediction based on drilling borehole data in the original geologic investigation report. The new insight of the approach is adopting a parametric modelling strategy to depict the stratum sequence and express the predicted soil property distribution. In addition, the drilling information logged in the geotechnical investigation report is sorted out and stored in DataFrame format to achieve data-driven modelling.

This study verifies a case study of the QXK+020~QXK+120 section in the Wuhan Lianghu tunnelling project. The case study confirms that 1) the geological cross-section model and the fitted groundwater surface can be efficiently generated within approximately 25 seconds; 2) at the same time, the overburden pressure on the crown of the correlating tunnel can be efficiently determined; and 3) the natural gravity distribution on the cutter head surface can be expressed through the greyscale map and helps the TBM operations. Although the prediction of it requires some hours, it can be arranged at other preparatory periods.

While the approach finally outputs the model in mesh type, rather than the Brep model, the nodes of mesh are capable of being exported as DataFrame for the subsequent work. Future work will focus on more practical demands of underground construction, such as load arrangements or constraint settings in the structure design.

https://doi.org/10.5194/isprs-annals-X-4-W2-2022-177-2022 | © Author(s) 2022. CC BY 4.0 License.

ACKNOWLEDGEMENTS

This study is supported by the National Natural Science Foundation of China (U21A20151) and the Major Scientific and Technological Innovation Project in Hubei Province (2020ACA006). The authors would like to thank Wuhan Municipal Engineering Design Research Institute Co., Ltd. for providing the case information and site survey information.

REFERENCES

Culí, L., Pujades, E., Vázquez-Suñé, E., & Jurado, A., 2016: Modelling of the EPB TBM shield tunnelling advance as a tool for geological characterization. *Tunnelling and Underground Space Technology*, 56, 12-21. doi.org/10.1016/j.tust.2016.02.017

Gong, W., Juang, C. H., Martin II, J. R., Tang, H., Wang, Q., & Huang, H., 2018: Probabilistic analysis of tunnel longitudinal performance based upon conditional random field simulation of soil properties. *Tunnelling and Underground Space Technology*, *73*, 1-14. doi.org/10.1016/j.tust.2017.11.026

Graciano, A., Rueda, A. J., & Feito, F. R. (2018). Real-time visualization of 3D terrains and subsurface geological structures. *Advances in Engineering Software*, 115, 314-326. doi.org/10.1016/j.advengsoft.2017.10.002

Han, L., Ye, G. L., Chen, J. J., Xia, X. H., & Wang, J. H., 2017: Pressures on the lining of a large shield tunnel with a small overburden: a case study. *Tunnelling and Underground Space Technology*, 64, 1-9. doi.org/10.1016/j.tust.2017.01.008

International Tunnelling Association., 2000: *Guidelines for the design of shield tunnel lining*. Tunnelling and Underground Space Technology.

Li, P., Shi, L., Liu, J., & Li, X., 2020: Complex Geological Modeling and Numerical and Digital Integration Based on iS3. *Journal of Chongqing Jiaotong University (Natural Science)*, 39, 3. doi.org/10.3969/j.issn.1674-0696.2020.03.19 (In Chinese)

Liu, L., Zhang, S., Cheng, Y. M., Liang, L., 2019: Advanced reliability analysis of slopes in spatially variable soils using multivariate adaptive regression splines. *Geoscience Frontiers*, *10*(2), 671-682. doi.org/10.1016/j.gsf.2018.03.013

Muzik, J., Vondráčková, T., Sitányiová, D., Plachý, J., Nývlt, V., 2015: Creation of 3D geological models using interpolation methods for numerical modelling. *Procedia Earth and Planetary Science*, 15, 25-30. doi.org/10.1016/j.proeps.2015.08.007

Ocak, I., 2014: A new approach for estimating the transverse surface settlement curve for twin tunnels in shallow and soft soils. *Environ Earth Sci*, 72, 2357–2367. doi.org/10.1007/s12665-014-3145-5

Sava, P., 2011: Micro-earthquake monitoring with sparsely sampled data. *Journal of Petroleum Exploration and Production Technology*, 1(1), 43-49. doi.org/10.1007/s13202-011-0005-7

Sun, S.; Li, L.; Wang, J.; Shi, S.; Song, S.; Fang, Z.; Ba, X.; Jin, H., 2018: Karst Development Mechanism and Characteristics Based on Comprehensive Exploration along Jinan Metro, China. *Sustainability* 2018, 10, 3383. doi.org/10.3390/su10103383

Wang, H., Wang, X., Wellmann, J. F., Liang, R. Y., 2018: Bayesian stochastic soil modeling framework using Gaussian Markov random fields. *ASCE-ASME Journal of Risk and Uncertainty in Engineering Systems, Part A: Civil Engineering*, 4(2), 04018014. doi.org/10.1061/AJRUA6.0000965

Wang, X., Li, Z., Wang, H., Rong, Q., Liang, R. Y., 2016: Probabilistic analysis of shield-driven tunnel in multiple strata considering stratigraphic uncertainty. *Structural safety*, 62, 88-100. doi.org/10.1016/j.strusafe.2016.06.007

Xu, G., He, C., Lu, D., Wang, S. 2019: The influence of longitudinal crack on mechanical behavior of shield tunnel lining in soft-hard composite strata. *Thin-Walled Structures*, *144*, 106282. doi.org/10.1016/j.tws.2019.106282

Yu, H., Tao, J., Qin, C., Liu, M., Xiao, D., Sun, H., Liu, C. 2022: A novel constrained dense convolutional autoencoder and DNN-based semi-supervised method for shield machine tunnel geological formation recognition. *Mechanical Systems and Signal Processing*, 165, 108353. doi.org/10.1016/j.ymssp.2021.108353

Zhang, C., Fu, J., Yang, J., Ou, X., Ye, X., Zhang, Y., 2018: Formulation and performance of grouting materials for underwater shield tunnel construction in karst ground. *Construction and Building Materials*, 187, 327-338. doi.org/10.1016/j.conbuildmat.2018.07.054

Zhang, Q., Zhu, H., 2018: Collaborative 3D geological modeling analysis based on multi-source data standard. *Engineering Geology*, *246*, 233-244. doi.org/10.1016/j.enggeo.2018.10.001